AIP | Review of Scientific Instruments

A low-temperature ultrahigh vacuum atomic force microscope for biological applications

Alexandra Radenovi, Eva Bystrenová, Laurent Libioulle, Mauro Taborelli, James A. DeRose, and Giovanni Dietler

Citation: Review of Scientific Instruments **74**, 1022 (2003); doi: 10.1063/1.1532840
View online: http://dx.doi.org/10.1063/1.1532840
View Table of Contents: http://scitation.aip.org/content/aip/journal/rsi/74/2?ver=pdfcov
Published by the AIP Publishing

A low-temperature ultrahigh vacuum atomic force microscope for biological applications

Alexandra Radenović, Eva Bystrenová,[a] Laurent Libioulle, Mauro Taborelli,[b] James A. DeRose,[c] and Giovanni Dietler
Institute of Condensed Matter Physics, University of Lausanne, CH-1015 Lausanne, Switzerland

(Received 20 May 2002; accepted 30 October 2002)

We present an atomic force microscope (AFM) for operation at low temperatures under ultrahigh vacuum conditions. It uses the laser beam deflection method to measure the bending of the cantilever. The four quadrant photodiode allows the detection of vertical and lateral forces. The AFM has been developed for studying biological samples. Images of deoxyribonucleic acid plasmids have been obtained in contact mode. © *2003 American Institute of Physics.*
[DOI: 10.1063/1.1532840]

I. INTRODUCTION

Nowadays, the atomic force microscope (AFM)[1] is successfully utilized to image a broad range of biological specimens because it can image nonconductive and soft material. Since the invention of the AFM, a lot of progress has been made in imaging biomolecules. However, high-resolution imaging has been achieved only in a very few cases.[2–5] The reasons why it is difficult to obtain high-resolution images are as follows: (a) the softness of fully hydrated macromolecules, which are easily deformed or damaged by the tip, (b) thermally induced motion of the macromolecules at room temperature, and (c) the aspect ratio of biomolecules compared to that of the tip. Operating the AFM at low temperature (cryo AFM) offers a solution to problems (a) and (b) just mentioned. Additionally, operating an AFM at low temperatures reduces the instrument noise.

At present, there are several other approaches for circumventing these problems when studying biological materials. For example, utilizing the AFM in tapping mode,[6] contact scanning in liquid solution,[7] or imaging of two-dimensional protein crystals.[2] This last approach is limited to macromolecules which can form close-packed flat patches on a substrate surface.

On the other hand, the cryo AFM appears to be the most promising approach, because it will work on all macromolecules and could become a general method in the future. Lowering the sample temperature will increase the mechanical stability of the molecules and will decrease its thermal induced motion. Simultaneously, a lower temperature will reduce the thermal induced motion of the cantilever reducing then the overall noise of the instrument. One has to admit that by this approach the biological sample is no longer in a physiological solution, a drawback that cryo-AFM shares with the electron microscope.

After these considerations, it seems reasonable that by lowering the temperature, one can gain resolution. Yet, the open question remains as to how low the temperature of the sample must be in order that the biomolecules are stiff. Infrared absorption measurements have shown that most of the proteins undergo a phase transition into a ''glasslike'' state when they are cooled below about 180 K.[8] Below this temperature, the protein is frozen into a rigid conformational state. Operating the AFM at liquid-nitrogen temperature is thus expected to be sufficient for studying the structure of biomacromolecules.[9]

II. INSTRUMENT DESIGN

The microscope system built in our laboratory is presented in Fig. 1. It consists of two chambers: the main chamber with the low-temperature AFM microscope and the preparation chamber, where the sample and tip can be cleaned and prepared. Furthermore, it has two cooled transfer rods for transferring the samples and the cantilevers in the preparation chamber or in the main chamber. The vacuum is generated by turbomolecular and ion pumps (base pressure is about 10^{-9} mbar). During the AFM measurements, no turbomolecular pump is running in order to prevent mechanical vibrations and the vacuum is maintained solely by the ion pumps.

The complete system is mounted on a frame supported by four pneumatic damping legs (Newport Ltd.). The frame is filled with sand to damp any internal vibrations. The AFM microscope is mechanically decoupled from the rest of the chamber by means of a second pneumatic damping stage and by the use of a very soft UHV bellow.

The Dewar system with the AFM head is schematically shown in Fig. 2(a). The outer cryostat is a hollow concentric cylinder that contains liquid nitrogen (LN_2) and acts as a cooled shielding screen. The inner cryostat can be filled either with LN_2 for measurements down to 77 K or with liquid helium for measurements down to 4.2 K. It has a capacity of 8.5 L and can keep the system at liquid helium temperature for approximately 9 h between subsequent refills. When the cooling medium is nitrogen, the hold time is more than three

[a]Electronic mail: Eva.Bystrenova@ipmc.unil.ch
[b]Presently at: CERN, Engineering Support and Technology Division, CH-1211 Geneva 23, Switzerland.
[c]Presently at: CYTION SA, Biopôle, Ch. des Croisettes 22, CH-1066 Epalinges, Switzerland.

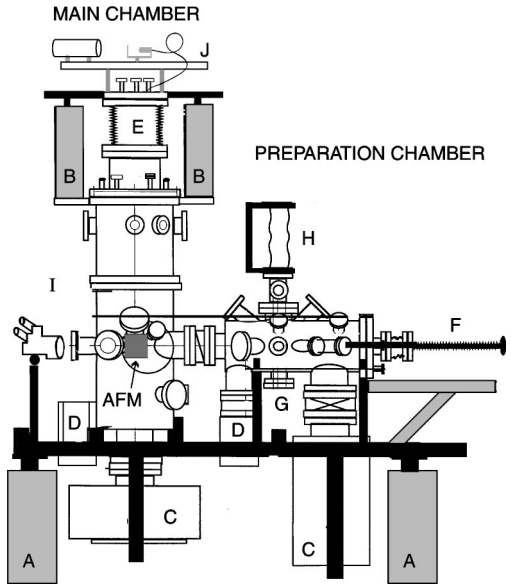

FIG. 1. The low-temperature ultrahigh vacuum atomic force microscope: (A) The first antivibration stage, pneumatic damping legs, (B) The second antivibration system, (C) Ion pumps, (D) Turbomolecular pumps, (E) Bellows support, (F) Transfer road, (G) Ion sputter gun, (H) Magnetron evaporator, (I) Optical microscope, and (J) He-Ne laser with optical fiber coupler.

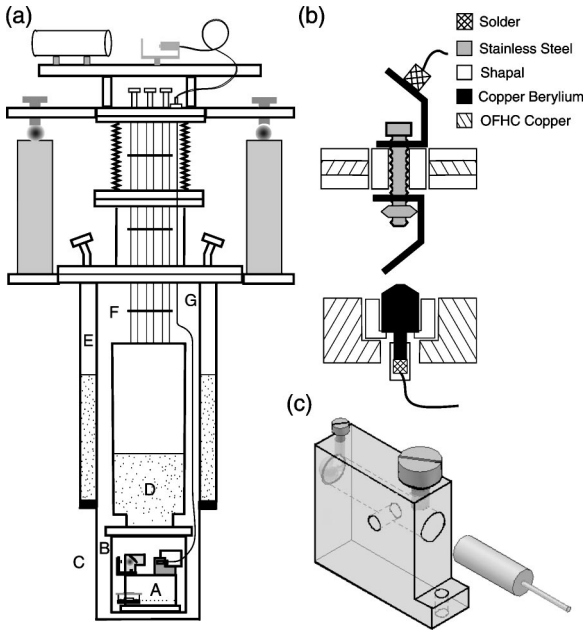

FIG. 2. (a). Schematic drawing of the main chamber: (A) AFM head, (B) First shield—copper box attached to the inner cryostat, (C) Second shield attached to the outer cryostat, (D) The inner cryostat, (E) The outer cryostat (F) System of copper radiation shields, and (G) Optical fiber. (b) The pin-spring system for electrical connections. (c) The aluminum housing for optical fiber.

days. Both home built cryostats are electropolished and silver painted after fabrication in order to lower the surface emissivity. Two copper shields are attached to the bottom of each cryostat to protect the AFM head against radiation. The electronic control unit of our microscope is the SPM-200 developed by RHK-Technology and it is interfaced to the AFM head by a home-built interface. The design of the AFM head is shown in Fig. 3. It was primarily guided by the goal to reach high resolution while imaging biological samples under UHV conditions and at low temperature. This limits the materials that can be used. Therefore, the central issues were vacuum and wide temperature range (4.2–400 K) compatibility.

The body of our microscope is made from oxygen free high conductivity (OFHC) copper block (dimensions 6 cm×8 cm×8 cm) in order to provide fast cooling. The microscope is electrically isolated via sapphire plates and held in place by two screws electrically isolated by shapal rings [Fig. 4.(G)]. Thus, the AFM mechanics can be easily transferred on an external setup for testing.

The inner cryostat has been fitted with twisted pair wires (phosphor bronze) and coaxial cables (stainless steel). In total, 35 electrical connections are needed to properly operate the microscope. Both materials used for the wires have been chosen to assure low thermal conductivity and low noise coming from electrical contacts. The electrical connections between the AFM mechanics and the connection wires are done through a ''pin–spring'' system as schematically drawn in Fig. 2(b). Two copper beryllium springs are held in the place with M1 stainless steel screws through an OFHC copper piece of the AFM head resting on the shapal base. The upper spring wire is soldered (UHV and cryo compatible solder). The lower spring is pushed toward the copper beryllium pin in the shapal mat inside the copper base. The wire is then soldered on to the bottom of the pin and placed in a teflon tube. This setup works very well even under a large temperature variation, it is UHV compatible, and operates as well as at high voltage or low amplitude signal voltage without any problems.

The choice of a suitable cantilever deflection detector was one of the most crucial decisions to make while designing the microscope. The methods of fiber optic interferometery[10] or piezoresistive cantilevers[11] have been proposed as the most simple to implement for low-temperature AFM, because they eliminate the necessity of fine mechanical adjustment after any change of temperature. However, these methods do not allow the measurement of the lateral force. Therefore, we have chosen the laser beam deflection method for detecting cantilever bending. A laser spot is reflected by the tip onto a four-quadrant photodiode which allows both vertical and lateral forces to be measured while scanning the samples, (see Fig. 4). The signal from the four-quadrant photodiode is transformed into different signals (A+B)-(C+D) for topography measurement or (A+C)-(B+D) for friction.

The laser beam deflection method requires precise focusing of the laser beam onto the cantilever tip. The laser beam is coupled into a single-mode optical fiber (length of 3.5 m and diameter of 125 μm), which is introduced inside the main chamber through a special home-made feedthrough [Fig. 2(G)]. We have chosen a single-mode fiber, because the shape and the direction of the emitted beam are fixed and decoupled from variations of the laser beam direction, which in turn reduces the beam intensity fluctuations.[12] In order to minimize spot intensity variations due to small vibrations of the fiber, which would be seen as a signal, we have placed the He–Ne laser (633 nm and 3 mW) and the fiber coupler

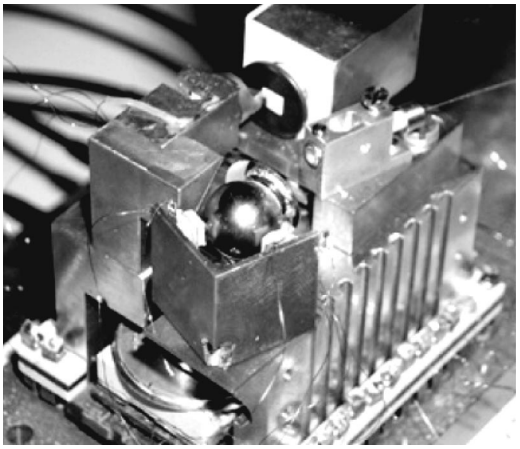

FIG. 3. Photograph of the AFM head.

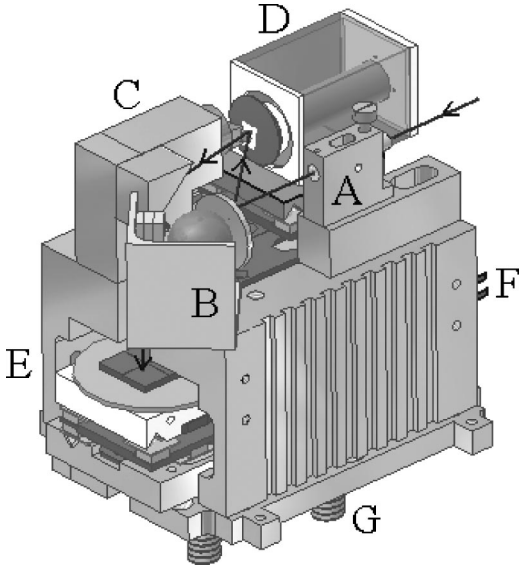

FIG. 4. The schematic drawing of AFM head. (A) Housing for optical fiber, (B) tilter, (C) tip holder stage with fix mirror, (D) scanner with sample holder, (E) photodiode on the slider, (F) thermometer, and (G) junction screws.

on the same stage as the inner cryostat [Fig. 1(J)].

Figure 2(c) shows the housing setup of the optical fiber. In order to easily position the end of the optical fiber in the AFM head, the fiber is glued into a ferrule. The optical fiber termination is polished and the ferrule is inserted into an aluminum housing holding a lens (Geltech 350550), which focuses the beam onto the end of the cantilever. The spot size on the cantilever is about 16 μm. The variation of the spot size with temperature (from 4 to 300 K) is approximately 7 μm due to defocusing by thermal expansion. The simple geometry of the housing allows one to easily change its angle, if necessary. When the fiber is removed and reinserted into the housing, a pin placed in front of the fiber termination precisely fixed the position in order to always have the same spot size on the cantilever.

In order to improve the signal-to-noise ratio, the gain of the photodiode preamplifier is set to 40×10^3 V/A and the laser spot intensity has been increased up to 700 μW on the output of the single mode optical fiber. The total noise on the topographic signal is about 1 mV peak to peak, including the noise generated by the laser itself, leading to an experimental sensitivity of our instrument in the *z* direction of about 0.5 Å.

For the precise adjustment of the position of the laser spot on to the cantilever, we have developed a rotating mirror on a compact three-axis spherical tilter [Fig. 4(B)], which holds a sphere with a mirror.[13] It allows very fine adjustment in all spatial directions (minimally up–down 0.018° and left–right 0.08° per 200 V). After transferring the cryogenic liquid and cooling down the system, it is necessary to readjust the spot on the cantilever. Using a long distance optical binocular [Fig. 1(I)] with a 40 cm focal length, we are able to observe the cantilever/sample region inside the chamber with fine resolution. To better visualize the cantilever a charge coupled device camera is fixed on the binocular microscope. A joystick controller is used to move the laser spot on to the cantilever by adjusting the rotating mirror.

The cantilever is fixed on a copper holder [Fig. 4(C)] on which it is kept in place by means of a clamp and a spring. The cantilever is tilted 14° with respect to the sample surface plane. We are using standard contact mode gold-coated cantilevers made of silicon nitride (Digital Instruments), which have been locally uncoated by focused ion beam milling leaving only the tip end coated. It is necessary to uncoat the levers, in order to avoid large bending during cooling induced by the difference between the thermal expansion coefficients of the gold film and the lever. A small part of the coating was left at the tip end of the cantilever in order to maximize light reflection. An alternative is to use uncoated Si cantilevers (NT MDT Co.) or double-sided gold chrome coated Si_3N_4 cantilevers (Olympus). The spring constant of these cantilevers is in range from 0.03 N/m to 0.3 N/m. The adhesion force observed for these cantilevers is 2–4 nN in the whole temperature range.

The reflected light beam from the cantilever is directed by a fixed mirror onto a four-quadrant photodiode placed inside the AFM mechanics. The photodiode (PIN-spot-9DMI, United Detector Technology) has been modified in order to work properly under vacuum and low-temperature conditions. We have removed its glass cover and extended the wire connections between the quadrants and the connecting pins. The photodiode is placed onto a slider,[14] which can be moved in two orthogonal directions.

The slider is made with two perpendicular stick and slip piezomotors and consists of two OFHC copper bases onto which are glued three shear piezoelectric plates for each base. A small sapphire sphere is glued on each piezoplate. Two sapphire spheres slide in a sapphire V-groove, while the third sphere slides on a sapphire plate. The shearpiezos are driven by a sawtooth voltage signal (550 $V_{\max}$ at a frequency of 1 kHz or less). This piezoelectric stepper motor allows precise adjustment of the photodiode in the two horizontal directions.

The single-tube scanner [Fig. 4(D)] is a 20 mm long piezoelectric tube (EBL 2, Staveley Sensors Inc.). The outer diameter is 6.35 mm resulting in a 16 μm maximum *XY* scan range and 3 μm maximum *Z* scan range for a $\pm$220 V voltage signal at room temperature. At 80 K, the sensitivity of the piezoelectric material is reduced by about 60%.[9] One end

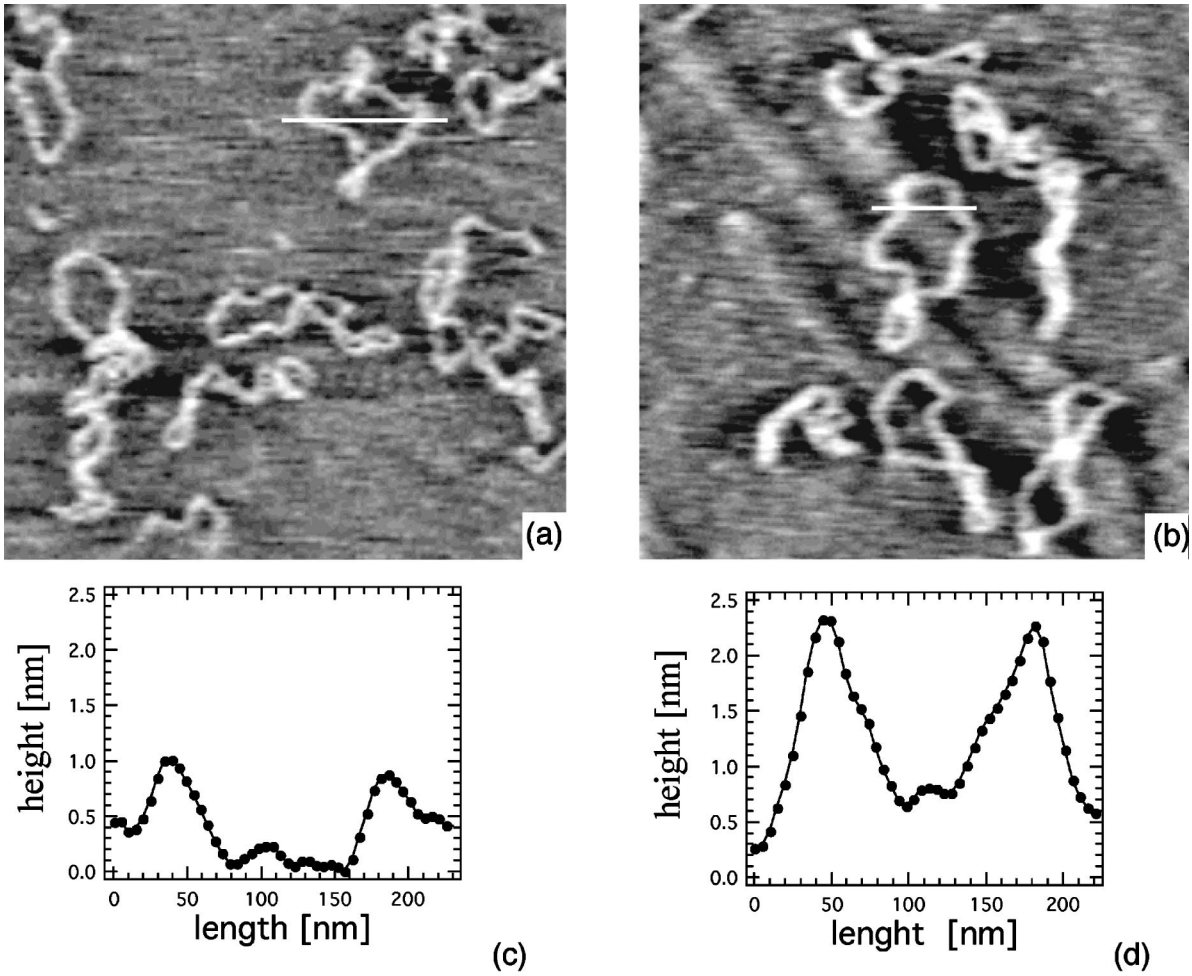

FIG. 5. CryoAFM images in contact mode of pUC19 DNA plasmids (a) under ambient conditions and (b) at low temperatures and in UHV. Both images are 1×1 μm. Corresponding line scan over the DNA plasmid under ambient conditions (c) and at low temperatures (d). Significant height difference is seen for the DNA plasmid.

of the tube is glued onto a machinable ceramic support and the other end is free and holds the metallic sample holder via a cobalt samarium magnet. The electrical connections are glued on the piezotube electrodes with conductive epoxy glue. The whole scanner is mounted on a slider stage (identical to the one used for the photodiode), which is performing the coarse approach of the sample toward the tip and is repositioning the sample horizontally in order to change the position of the scanned area.

III. EXPERIMENTAL RESULTS AND DISCUSSION

The AFM is of great interest for imaging biological samples because it achieves high resolution in all three dimensions, which is not easily the case for other techniques such as electron microscopy. Therefore, we recorded contact mode images of pUC 19 [a deoxyribonucleic acid (DNA) plasmid] at 180 K. The plasmids were purified according to the procedure described in Ref. 15. Samples of DNA were prepared by the following procedure:[16] the stock plasmid DNA solution was diluted in a TBE buffer at a *p*H of 7.5 with the addition of 10 mM $MgCl_2$. The solution was then deposited directly onto freshly cleaved mica for a 2 min incubation, and then the mica was gently rinsed with ultrahigh-purity water and dried with air.

The cooling process is as follows: LN_2 is poured into both cryostats. The temperature reaches 80 K as measured by a thermosensor (Lake Shore Inc.) on the AFM head [Fig. 4(F)]. This base temperature is reached in 90 min. Due to the boiling of the nitrogen inside the inner cryostat, an higher level of noise is observed under cryogenic conditions. Once all liquid from the inner cryostat has evaporated and the temperature starts to increase slightly, the AFM gives the best performance. The system requires approximately 20 h to reach room temperature. The temperature increases by approximately 0.1 K/min and we did not observe any kind of drift or nonstability in the images even at very slow scanning speed (down to 0.5 Hz).

The AFM images were flattened off-line by a scanning probe image processor (Image Metrology ApS) to remove the background noise from cantilever bending fluctuations and laser intensity fluctuations.

Typical AFM results on DNA plasmid samples are shown in Fig. 5, where we present topographic images recorded at room temperature and at 180 K. It is interesting to note that, in both pictures, one can see partly condensed, supercoiled, and relaxed plasmids of DNA.

Figures 5(c) and 5(d) show cross sections of the plasmids. At room temperature, the height observed throughout

the image is less than 1 nm compared to the value of 2–3 nm known from crystallography.[17] By lowering the temperature to 180 K, DNA molecules become much stiffer and their true height of 2 nm is more easily observed as shown in Fig. 5(d). A more detailed analysis on a larger number of plasmids gives an average height at room temperature of (0.6 ± 0.4) nm, while at 180 K, the average height is (2.2 ± 0.6) nm. Since the commercial cantilevers used in our measurements have a nominal tip radius of 20–60 nm we observed a quite large tip–sample convolution and a lateral resolution about 20–30 nm even with a properly adjusted adhesion force between the tip and sample (2–4 nN).[18] Improvements should be possible if ultrasharp tips are used.

Up until now, nearly all AFM measurements on DNA have shown a much reduced height in the range of 1–1.5 nm (Ref. 19) with the exception of Shao *et al.*[20] using an AFM operating in nitrogen vapor. This reduced height was attributed to the condensation of salt and other solutes onto the surface in the vicinity of the DNA during the drying process. In this case, the height of DNA should be lower, and the width of the DNA strand should increase, which was not observed in our measurements. We can not exclude the presence of few layers of the water on the surface of the sample. In order to eliminate it, several improvements could be done, for example, using hydrophobic specimens or preparing the samples inside the UHV chamber.

Based on these results, it seems promising that the low-temperature UHV AFM will open new possibilities for studying biological samples and that it will be possible to better resolve their structure which can be related to the their function.

ACKNOWLEDGMENTS

The authors would like to thank the entire machinist's team at the University of Lausanne for their continuous help and Francesco Valle for sample preparation. This work was partially funded by the Swiss National Science Foundation under Grant Nos. 21-050805.97, 2000-57133.99, and 2000-065160.00.

[1] G. Binnig, C. F. Quate, and A. C. Gerber, Phys. Rev. Lett. **56**, 930 (1986).
[2] S. Scheuring *et al.*, Single Molecules **2**, 59 (2001).
[3] J. Mou, D. Czajkowsky, Y. Zhang, and Z. Shao, FEBS Lett. **371**, 279 (1993).
[4] Z. Shao and Y. Zhang, Ultramicroscopy **66**, 141 (1996).
[5] Z. Shao, News Physiol. Sci. **14**, 142 (1999).
[6] F. Valle *et al.*, J. Microsc. **203**, 195 (2001).
[7] D. J. Möller *et al.*, EMBO J. **16**, 2547 (1997).
[8] I. E. T. Iben, D. Braunstein, W. Doster *et al.*, Phys. Rev. Lett. **62**, 1916 (1989).
[9] J. Mou, J. Yang, and Z. Shao, Rev. Sci. Instrum. **64**, 1483 (1993).
[10] D. Rugar *et al.*, Rev. Sci. Instrum. **59**, 2337 (1988).
[11] R. E. Thomson, Rev. Sci. Instrum. **70**, 3369 (1999).
[12] R. C. Barrett and C. F. Quate, J. Vac. Sci. Technol. A **8**, 400 (1990).
[13] L. Howald, H. Rudin, and H.-J. Guntherogt, Rev. Sci. Instrum. **63**, 3909 (1992).
[14] D. W. Pohl, Rev. Sci. Instrum. **58**, 54 (1987).
[15] V. Viglasky, M. Antalik, J. Adamcik, and D. Podhradsky, Nucleic Acids Res. **28**, e51 (2000).
[16] L. H. Pope *et al.*, J. Microsc. **199**, 68 (2000).
[17] J. D. Watson and F. H. C. Crick, Nature (London) **171**, 737 (1953).
[18] J. Yang, J. Mou, J.-Y Yuan, and Z. Shao, J. Microsc. **182**, 106 (1996).
[19] H. G. Hansma, I. Revenko, K. Kim, and D. E. Laney, Nucleic Acids Res. **24**, 713 (1996).
[20] Z. Shao, J. Yang, and A. P. Somlyo, Annu. Rev. Cell Dev. Biol. **11**, 241 (1995).